JOURNAL OF Materials CHEMISTRY

A new hydrothermal fluoro-zircon†

Rémi Valéro,[a] Luc Delmotte,[a] Jean Louis Paillaud,[a] Bernard Durand,[a] Jean Louis Guth[a] and Thierry Chopin[b]

[a] *Laboratoire de Matériaux Minéraux, UPRES-A7016, ENSCMu, 3 rue A. Werner, 68093 Mulhouse cedex, France. E-mail: BE.Durand@univ-mulhouse.fr*
[b] *Centre de Recherches Rhône-Poulenc, 52 rue de la Haie Coq, 93308 Aubervilliers, France*

Received 16th April 1998, Accepted 28th July 1998

A zircon exhibiting original properties was synthesized under autogenous pressure at 150 °C for a few tens of hours. Silicon vacancies in the form of tetrahedral nests $[F_n(OH)_{4-n}]$ were identified by coupling ^1H NMR CRAMPS and thermogravimetry. A Rietveld refinement of the structure was performed. The mechanism of the hydrothermal synthesis involves heterocondensation reactions between the $Si(OH)_4$ species and a fluoro-zirconium complex rich in fluorine. Annealing of this fluoro-zircon above 500 °C produces, according to the heating profile, either monoclinic or tetragonal zirconia with a plate-like morphology having an acicular network texture.

Zircon is used as refractory material. Because of its low thermal expansion coefficient,[1] the mechanical strength of sintered bodies is not altered, even at temperatures higher than 1400 °C.[2,3] When prepared with a high specific surface area, it may find applications in heterogeneous acid catalysis.

Zircon was first synthesized in 1865 by solid state reaction at about 1500 °C.[4] Nowadays, in order to obtain powders of better quality, two main methods have been developed, the sol–gel route from alkoxide precursors[5,6] and hydrothermal synthesis. A hundred years ago, Von Chrustchoff[7] indicated the presence of zircon in the reaction products of SiO_2–ZrO_2 mixtures inside an autoclave in the presence of water and under autogenous pressure. Fifty years ago, Frondel *et al.*[8] showed that zircon could be obtained from gelatinous zirconia and silica, by hydrothermal treatment at 400 °C for 168 h at 1000 bar pressure. The temperature and the pressure were respectively decreased to 150 °C and 4.8 bar by adding traces of ZrF_4; however the reaction still needed 500 h. More recently, several studies were carried out by varying the synthesis parameters (temperature, pressure, time, pH, nature of Si and Zr sources, *etc.*).[9–13]

From bibliographical information, it was concluded that hydrothermal synthesis of zircon at temperatures below 200 °C is possible but often requires very long times. Yet, the addition of fluoride ions to the medium seemed to raise the reaction rate. So, a thorough study of the hydrothermal synthesis of zircon in fluoride medium and under autogenous pressure was entered upon in 1996.[14] Syntheses were carried out at 150 °C for times in the range 24–144 h, after an investigation of the influence of fluoride ions on the solubility of ZrO_2, SiO_2 and $ZrSiO_4$ in the hydrothermal media,[15] and a spectroscopic characterisation of the nature of the dissolved species when they were unknown.[16]

New zircons with original morphologies, named 'Zircons B', were obtained in basic media.[17] Fluoride acts only as a crystallization catalyst and the powders essentially contain no fluorine. Thin plate-shaped crystallites are formed by reaction between the dissolved monomeric silicon species $Si(OH)_3O^-$ and dissolved zirconium polymers with Zr–O–Zr oxobridges. Then, depending on the time and the fluoride concentration, the gathering of crystallites builds either layered platelets by stacking of crystallites or ellipsoïdal agglomerates of platelets (Fig. 1). It is thought that the growth of ellipsoïds involves a combination of two processes, one allowing the growth of platelets and the other being responsible for the formation of surface heterogeneities on the platelets. Under suitable conditions, specific surface areas as high as 200 $m^2\,g^{-1}$ are achieved and samples exhibit excellent thermal stability, 50% being maintained after annealing at 800 °C for 72 h, *i.e.*, 100 $m^2\,g^{-1}$.

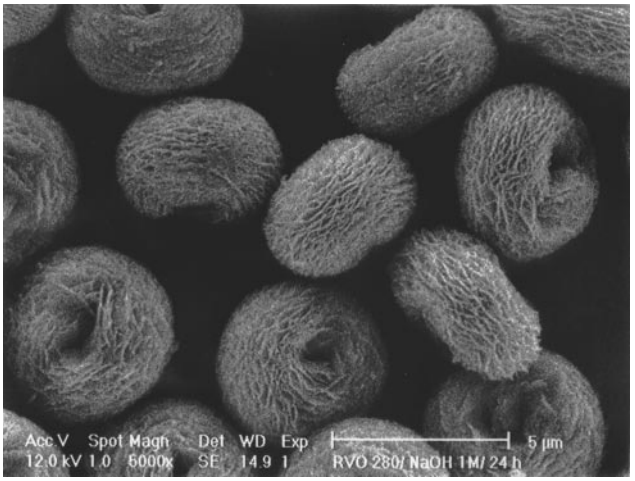

Fig. 1 SEM micrograph of a zircon B powder (F/Zr = 2, Si/Zr = 1, pH = 9).

The characteristics of the zircons synthesized in acid media depended mainly upon the fluoride concentration and the pH value. Two kinds of zircons were distinguished. (i) the 'Zircons C' are obtained in the areas where the solubilities of the zirconium and silicon sources are low and the fluorinated complexes of zirconium are poor in fluorine, *i.e.*, low fluoride concentration, whatever the acid pH [with the exceptions of pH *ca.* 2, or high fluoride concentration and very weakly acid pH (range 5–7)]. They are characterised by symmetrical SiO_4 tetrahedra, low F and OH contents mainly in the form of $[(OH)_3F]$ nests and a morphology in layered coils (Fig. 2). (ii) the 'Zircons A' are obtained in the areas where the solubilities of the zirconium and silicon sources are high and the fluorinated complexes of zircon are rich in fluorine, *i.e.*, high fluoride concentration and acid pH in the range 0–5. They are characterised by asymmetrical SiO_4 tetrahedra and high OH and F contents in the form of $[F_n(OH)_{4-n}]$ tetrahedral nests.

The possibility of incorporation of F and OH in the structure

†Basis of the presentation given at Materials Chemistry Discussion No. 1, 24–26 September 1998, ICMCB, University of Bordeaux, France.

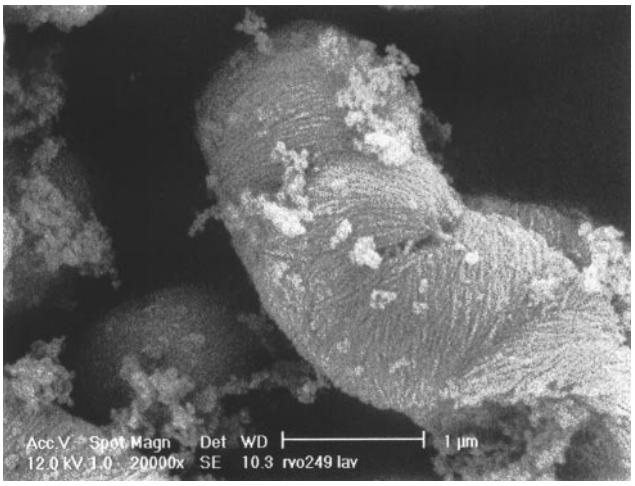

Fig. 2 SEM micrograph of a zircon C powder (F/Zr = 0.6, Si/Zr = 1, pH = 0).

of zircon was previously mentioned by Frondel *et al.*[8] and Caruba *et al.*[9,18] for syntheses carried out at pressure (700–1000 bar) considerably higher than autogenous.

The present paper deals with the synthesis and the characterisation of A type zircons.

Experimental

Procedure

The hydrothermal syntheses were performed in Teflon-lined stainless-steel autoclaves at 150 °C and various times in the range 24–144 h, under autogenous pressure. The starting materials were amorphous silica (Aerosil 130, from Degussa), zirconium oxychloride ($ZrOCl_2 \cdot 8H_2O$, from Fluka), hydrofluoric acid (HF 40 wt% from Prolabo) and distilled water. The reactions of two mixtures were mainly studied:

$$1\ ZrO_2 : 1\ SiO_2 : 1250\ H_2O : 2\ HF \text{ (Sample a)}$$
$$1\ ZrO_2 : 0.3\ SiO_2 : 350\ H_2O : 3\ HF \text{ (Sample b)}$$

The hydrothermal medium was stirred at room temperature until homogenous. The pH was then adjusted to 2 by adding aqueous ammonia before the syntheses were carried out. No significant pH change occurred during the thermal treatment. The microcrystalline products were filtered, washed with distilled water and finally either dried at room temperature or oven-dried at 120 °C for 48 h.

Characterisation

The silicon, zirconium and fluorine contents of powders were determined respectively by atomic absorption (Varian AAG), colorimetry with 8-hydroxiquinolinol[19] and by means of a specific electrode.

The X-ray diffraction (XRD) patterns for phase identification were recorded on a Philips PW 1800 variable entrance slit diffractometer using Cu-Kα radiation in the 2θ range 5–50°, at a scan rate of 1°C min^{-1}. For the Rietveld refinements, the XRD powder data were collected on a Stoe Stadi-P diffractometer equipped with a linear position-sensitive detector in Debye-Scherer geometry 6° in 2θ and employing Ge monochromated Cu-Kα_1 radiation.

The infrared spectra were recorded on a Perkin Elmer spectrometer with KBr pellets (1 mg of zircon per 300 mg of KBr).

The NMR spectra were obtained by means of Bruker spectrometers, either MSL 300 (^{29}Si MAS NMR) or DSX 400 (^{19}F and ^{1}H MAS NMR; ^{1}H CRAMPS NMR). Working parameters are given in Table 1. The chemical shifts were referenced to tetramethylsilane (TMS) for ^{1}H and ^{29}Si, and to $CFCl_3$ for ^{19}F.

The scanning electron micrographs (SEM) were obtained on a Philips XL 30 microscope. Transmission electron microscopy (TEM) observations were performed on a Philips CM 30 instrument operating at 30 kV.

The thermal analysis was carried out from ambient to 850 °C using a Setaram instrument under the following conditions: TGA: heating rate 4 °C min^{-1}, air flow 0.2 l h^{-1}; DTA: heating rate 10 °C min^{-1}.

Results

Chemical analysis and EDX data

For both samples, the chemical composition determination revealed (Table 2) Si/Zr molar ratios strongly lower than those initially introduced in the hydrothermal reaction medium and the presence of significant amounts of fluorine. The silicon defects and fluorine contents were the highest as the ratio Si/Zr in the medium was decreased and as the fluoride concentration [F^-] was raised.

The annealing of sample a for 12 h at 450 and 850 °C involved a progressive decrease of its silicon and fluorine contents. Chemical analysis needed a preliminary dissolution of the powder and gave an average value of the Si/Zr ratio of the sample. Energy dispersion of X-rays experiments, carried out with the electron beam centered in crystallized areas of the sample, led to smaller Si/Zr ratios. The discrepancy indicated heterogeneities in the chemical composition of the powder between crystallized and amorphous areas.

The release of silicon during annealing was corroborated by dissolution of the evolved gases in 1 M sodium hydroxide and spectrometric analysis of the silicon content in the solution.

Phase identification

The XRD patterns of samples a and b were similar but different from the pattern of a classic zircon (zircon from Aldrich, ICDD file no. 6–626) by the abnormal relative intensities of peaks (101), (211), (112), (301) and (103) principally (Fig. 3). It was checked that the phenomenon was not caused by a preferential orientation, operating with a Debye–Scherrer camera. The relative intensity of the (101) peak seemed the most significant as the crystallization rate and the fluorine contents of zircons A were high.

Either monoclinic or tetragonal zirconia were identified in XRD patterns of sample a annealed at 750 °C for 12 h, depending on the heating profile (Fig. 4). When 750 °C was reached in one step at a rate of 750 °C h^{-1}, monoclinic zirconia was directly formed and some zircon remained, while tetragonal zirconia crystallized when the heating at the same rate was interrupted by holding for 4 h at 200, 370, 540 and 650 °C. The transformation of zircon into finely crystallized tetragonal zirconia was also investigated using a Guinier heating camera from 32–752 °C with increments of 45 °C. The amorphization of zircon was observed at about 350 °C, preceded by a small contraction of (200) lattice planes and the crystallization of tetragonal ZrO_2 began near 480 °C.

Infrared spectroscopy

Compared to that of classic zircon, the infrared spectra of samples a and b were characterised (Fig. 5) by a decrease of the intensity of the bands attributed to asymmetrical vibrations in SiO_4 tetrahedra (615 and 1000 cm^{-1}). This was attributed to the presence of asymetrical tetrahedra in A type zircons.

Moreover, the IR spectra of samples a and b were characterised by: (i) the presence of a narrow and strong band at 3700 cm^{-1} indicating the presence of OH groups in the structure; (ii) the absence of a narrow band at 1625 cm^{-1} and

Table 1 Working parameters in NMR of solids

Parameter	^{29}Si MAS NMR Bruker MSL 300	^{19}F and ^{1}H MAS NMR Bruker DSX 400	^{1}H CRAMPS NMR Bruker DSX 400
Frequency/MHz	59.6	376/400	400
Spinning rate/kHz	8	15	2
Pulse time (p/2)/ms	4	6	1.84
Recycle delay/s	360	6	45
Accumulation	60	10	60

Table 2 Chemical compositions (molar ratios) of samples a and b, influence of annealing of sample a at 450 and 800 °C for 12 h

Sample	Si/Zr EDX[d]	Si/Zr C.A.[f]	F/Zr C.A.[f]
a (i)[a]	0.31 (0.06)	0.40 (0.04)	1.75 (0.09)
(ii)[b]	—[e]	0.37 (0.04)	0.95 (0.06)
(iii)[c]	0.10 (0.02)	0.25 (0.02)	0.10 (0.06)
b[a]	—[e]	0.17 (0.02)	1.81 (0.11)

[a]As prepared. [b]Annealed at 450 °C for 12 h. [c]Annealed at 800 °C for 12 h. [d]EDX: energy dispersion of X-rays. [e]Not determined. [f]C.A.: chemical analysis.

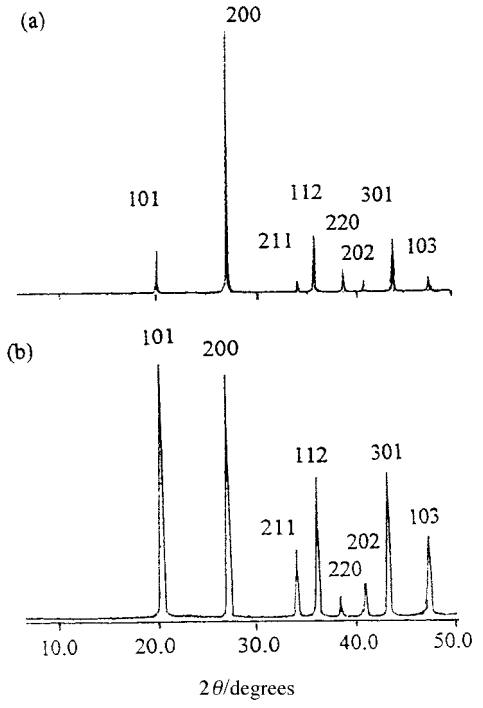

Fig. 3 XRD patterns (Cu-Kα radiation): (a) classic zircon, (b) hydrothermal fluorozircon sample a.

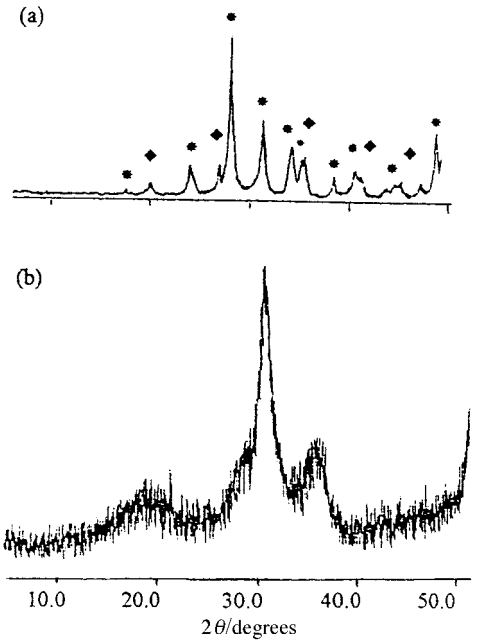

Fig. 4 XRD patterns (Cu-Kα radiation) of sample a annealed at 750 °C: (a) single step heating, (b) multi-step heating; (*) zircon, (◆) monoclinic zirconia.

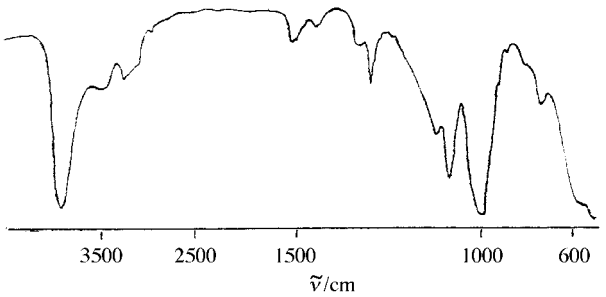

Fig. 5 IR transmission spectrum of sample a.

of a large band at 3500 cm^{-1} showing the absence of structural water in the solid; (iii) the presence of bands with low intensities in the range 1300–1500 cm^{-1}; in particular the band located at 1425 cm^{-1} could be attributed to the presence of adsorbed water; it vanished on oven-drying at 120 °C for 48 h.

Consequently, it was concluded that the dried powder contained only OH groups in its structure.

Morphological investigations

The SEM micrographs of the samples a and b (Fig. 6) revealed a platelet shaped morphology. The square platelets were micron sized and their thickness was increased by increasing $[F^-]$ and decreasing the Si/Zr molar ratio in the hydrothermal medium.

On the TEM micrograph of sample a annealed at 750 °C for 12 h (Fig. 7), it was observed that the transformation of zircon into monoclinic zirconia did not change the platelet morphology, but strongly altered the texture of each platelet. A network of zirconia needles, about 10×100 nm in size, was built and the orientation of the needles was related to the two mean crystallographic directions of the zircon platelet. Some silica drops were also noticed in the micrograph. The presence of amorphous silica, surrounding the zirconia needles, was more clearly seen in the HRTEM micrograph (Fig. 8).

Nuclear magnetic resonance studies

Comparison between the ^{29}Si MAS NMR spectra of sample a and classic zircon showed a small shift and a broadening of the silicon signal for sample a (Fig. 9). It was concluded that silicon was more screened in zircons A than in classic zircon and the change was attributed to an opening of the bond angles Si–O–Zr.

The ^{19}F MAS NMR spectrum of sample a was similar to that of a fluoro-zirconium germanate synthesized using the

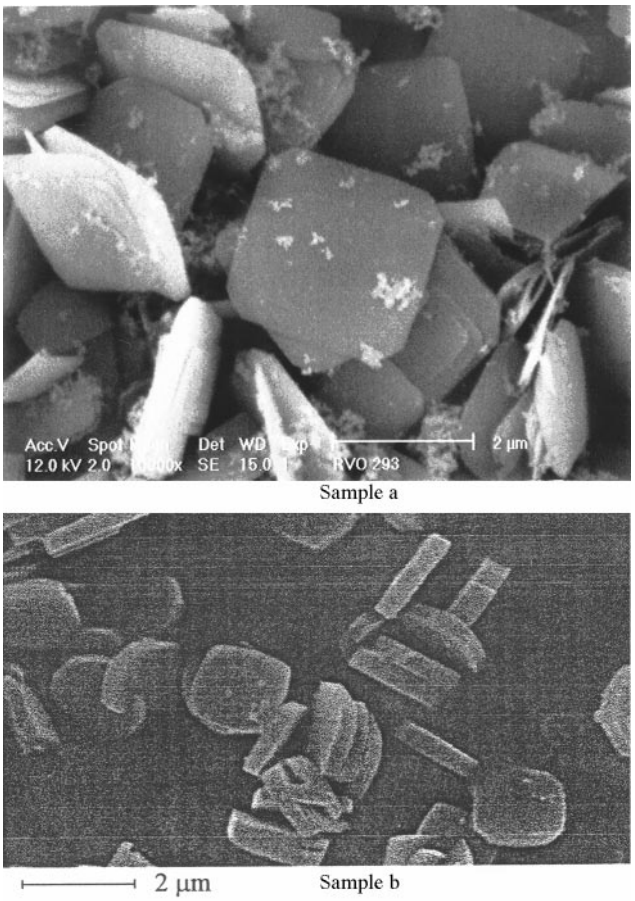

Fig. 6 SEM micrographs of hydrothermal fluoro-zircon samples a and b.

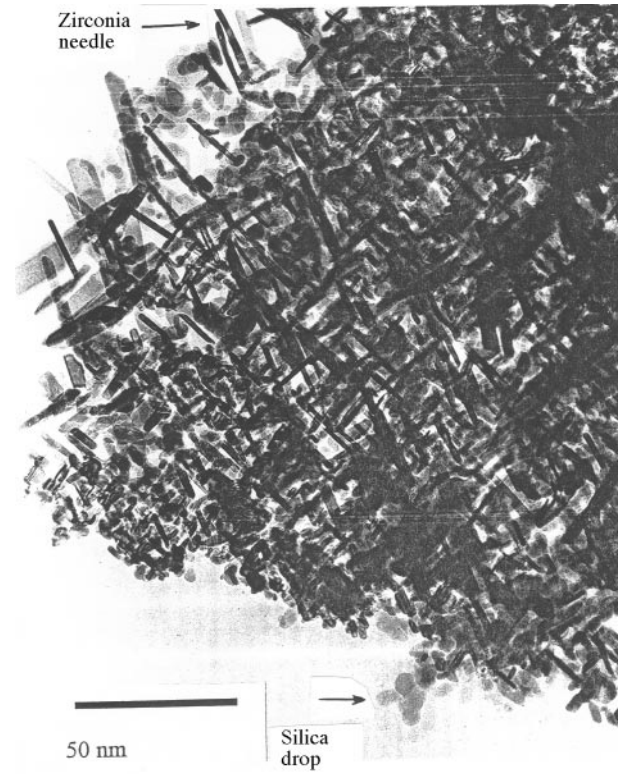

Fig. 7 TEM micrograph of sample a annealed at 750 °C.

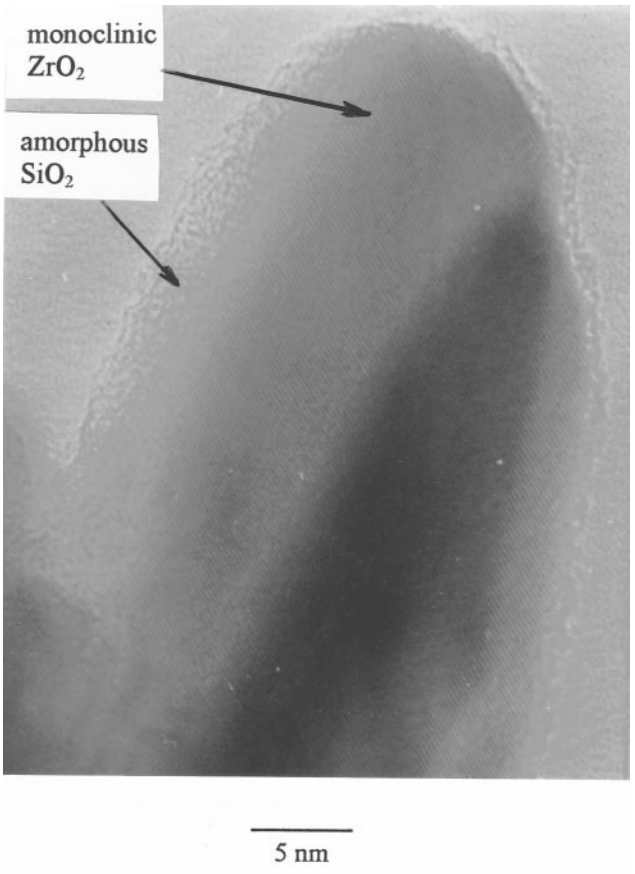

Fig. 8 HRTEM micrograph of sample a annealed at 750 °C.

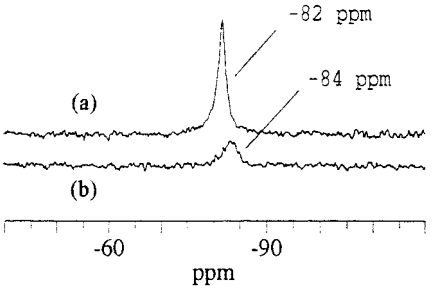

Fig. 9 ^{29}Si MAS NMR spectra: (a) classic zircon, (b) hydrothermal fluoro-zircon, sample a.

same procedure (Fig. 10). Consequently, the fluorine atoms were localised in the same sites in both compounds and were only bonded to zirconium atoms.

The ^{1}H MAS NMR spectrum of sample a [Fig. 11(a)] was characterised by a very broad signal, due probably to homo- and heteronuclear interactions. A better resolution was obtained using CRAMPS NMR for which three signals were identified in the spectrum [Fig. 11(b)]: (i) a broad signal extended over 10 ppm attributed to heteronuclear dipolar interactions between fluorine and hydrogen atoms; (ii) a sharp signal where heteronuclear interactions were very weak; it was related to protons inside tetrahedra poor in fluorine, assuming that tetrahedra containing only hydroxyl groups do not exist in the structure; (iii) a moderately broad signal extended over about 4 ppm which could be attributed to both hetero- and homonuclear interactions, the heteronuclear one still being efficient.

Thermogravimetric and differential thermal analyses

The calcination of zircons A, at a rate of 240 °C h^{-1}, involved relative weight losses of about 25% for sample a and 30% for

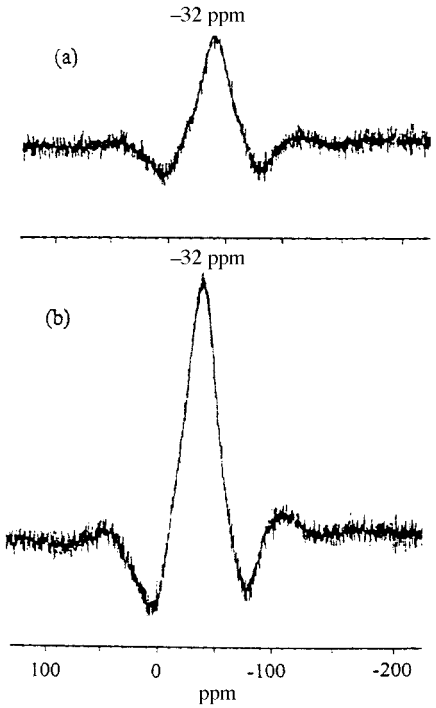

Fig. 10 ^{19}F MAS NMR spectra: (a) fluoro-zircon, sample a, (b) fluoro-zirconium germanate.

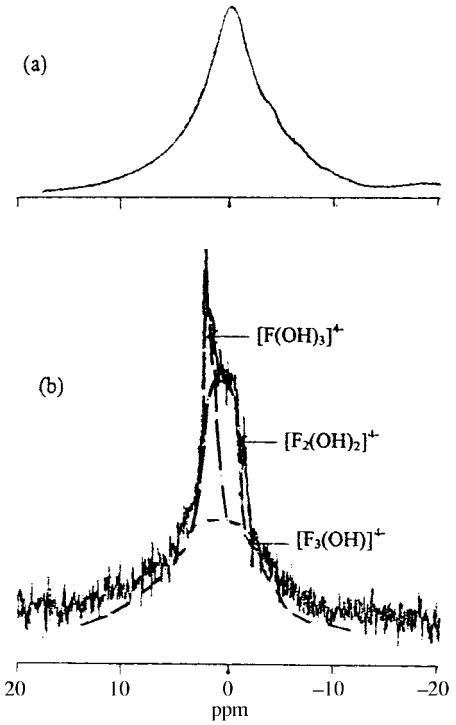

Fig. 11 ^{1}H NMR spectra of sample a: (a) MAS NMR, (b) CRAMPS NMR.

sample b occurring apparently in three steps (Fig. 12). The decrease of silicon and the increase of fluorine contents lowered the temperatures of the first two steps while it strongly raised the temperature and the magnitude of the third one. Hydrofluoric acid and silicon tetrafluoride were identified in the evolved gases. A significant endotherm was noticed in the DTA curve of sample a at about 530 °C (heating rate 600 °C h^{-1}) and attributed to the crystallization of monoclinic zirconia (Fig. 13). The peak occurred after the second weight loss and its temperature decreased linearly with the lowering of the Si/Zr ratio in the hydrothermal medium.

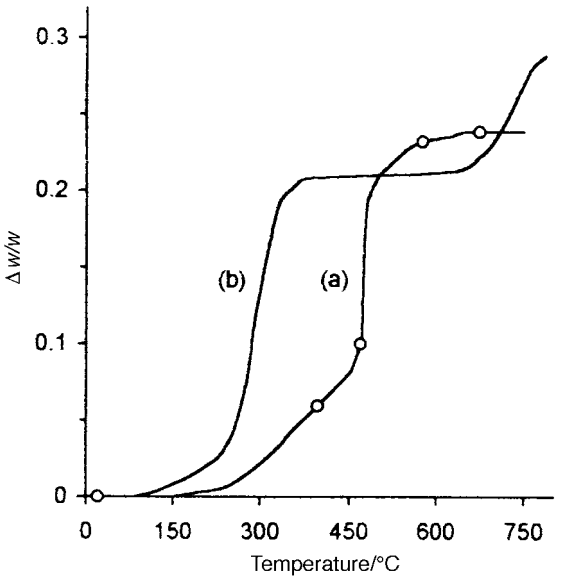

Fig. 12 Thermogravimetric curve of fluoro-zircons A: (a) sample a, (b) sample b; (○) points corresponding to the ^{1}H NMR spectra of Fig. 13.

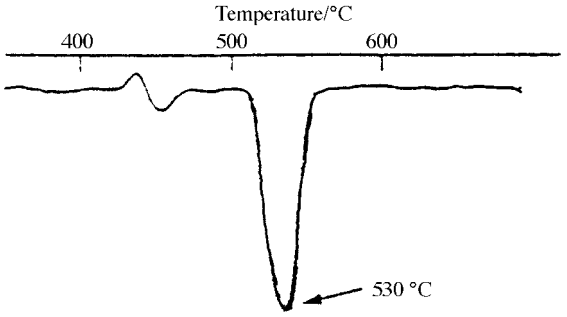

Fig. 13 DTA endothermic peak of crystallisation of monoclinic zirconia for sample a.

Discussion

From the above data, it was assumed that the structure of zircons A, characterised by silicon defects and significant proportions of fluorine, could be described by replacing, in the classic stoichiometric zircon structure, some SiO_4 tetrahedra by tetrahedral nests $[F_n(OH)_{4-n}]$ and that the transformation of zircons A into zirconia upon annealing, involved the progressive destruction of these nests. Convincing proof was obtained by coupling ^{1}H CRAMPS NMR and thermogravimetry and by Rietveld refinement of the structure.

Coupled ^{1}H CRAMPS NMR and thermogravimetry

^{1}H CRAMPS NMR spectra of sample a were recorded at various temperatures (Fig. 14) selected on the thermogravimetric curve (Fig. 12). The alteration of the ^{1}H NMR signal between room temperature and 470 °C, *i.e.*, during the first weight loss, came from the progressive disappearance of the broad and moderately broad peaks identified in the signal at room temperature [Fig. 11(b)] and attributed respectively to heteronuclear interactions and to the combination of homo- and heteronuclear interactions. The release of HF and SiF_4 was evidenced. Consequently, the first weight loss was indicative of the progressive destruction of $[F_3(OH)]$ (broad signal, heteronuclear interaction) and $[F_2(OH)_2]$ (moderately broad

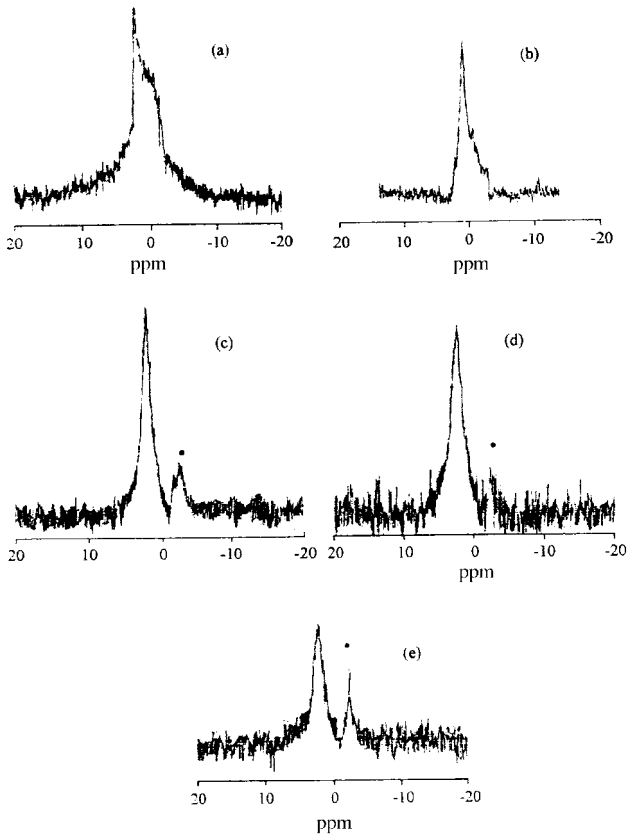

Fig. 14 Influence of annealing on the ^1H CRAMPS NMR spectrum of sample a: (a) room temperature, (b) 400 °C, (c) 470 °C, (d) 550 °C, (e) 675 °C; (●) NMR probe signal.

signal, homo- and heteronuclear interactions) nests. In the temperature range 470–550 °C, no change was noticed in the NMR signal whereas the thermogravimetric curve showed a sharp significant weight loss. So, the loss could not be related to the departure of OH groups, but only to the destruction of $[F_4]$ nests with the evolution of SiF_4. The alteration of the NMR signal between 550 and 675 °C corresponded to a decrease of the magnitude of the sharp peak. The third small weight loss was then attributed to the destruction of poorly fluorinated nests $[F(OH)_3]$ producing mainly homonuclear dipolar interactions.

Considering the existence of these nests and taking into account the chemical analysis and thermogravimetrical data, the following formula was calculated for sample a: $Zr(SiO_4)_{0.3}\{[F_4]_{0.3}[F_3(OH)]_{0.2}[F_2(OH)_2]_{0.3}[F(OH)_3]_{0.2}\}_{0.7}$, or in short $ZrSi_{0.3}O_{1.2}F_{1.82}(OH)_{0.98}$.

The transformation of the fluoro-zircon into zirconia concorded with the following equation giving a calculated weight loss (24.8%) in good agreement with the experimental one (25%):

$$ZrSi_{0.3}O_{1.2}F_{1.82}(OH)_{0.98} \rightarrow ZrO_2 + 0.09\ SiO_2 + 0.21\ SiF_4 + 0.98\ HF$$

From a similar analysis, it was concluded that, in sample b, the increase of the fluorine content and the decrease of the silicon content corresponded to a lowering of the proportions of $[F_3(OH)]$ and $[F_2(OH)_2]$ nests and to an increase of the proportion of $[F_4]$ nests; the three kinds being destroyed at a lower temperature. An increase of the proportion of $[F(OH)_3]$ nests was also noticed and they seemed to be destroyed at higher temperature.

Rietveld refinement

The collection of XRD data was treated using the GSAS suite of programs[20] and the initial model was taken from the previously reported classic zircon structure.[21] The refinement was initiated on the space group $I4_1/amd$.

Oxygen and fluorine atoms occupy the same sites, so their corresponding occupancy factors were fixed according to the chemical analysis. The full data will be published elsewhere[22] and only the main results are reported here (Table 3).

The structure of sample a was refined with a very satisfactory reliability factor $R_f = 0.0183$ and that of sample b with $R_f = 0.0387$. The replacement of SiO_4 tetrahedra of classic zircon by tetrahedral nests $[F_n(OH)_{4-n}]$ decreased the tetragonality c/a. The greater the number of replaced SiO_4, the smaller the c parameter and the higher the a parameter. The remaining SiO_4 tetrahedra were distorted.

Table 3 Rietveld refinement data

		Fluoro-zircon samples	
	Classic zircon	a	b
Lattice parameter/Å			
a	6.6164(5)	6.64025(3)	6.64821(2)
c	6.0150(5)	5.92625(6)	5.90758(4)
Bond length/Å			
Si–O	1.622(1)	1.65412(1)	1.6600(15)
Zr–O(F)	2.268(1)	2.24400(2)	2.2312(14)
	2.131(1)	2.11495(1)	2.1152(16)
Bond angle/°			
O–Si–O	116.06(1)	115.91(7)	116.08(6)
	97.0(1)	97.23(1)	96.93(1)

Conclusion

The hydrothermal synthesis at 150 °C for a few tens of hours under autogenous pressure, in acid medium containing signifi-

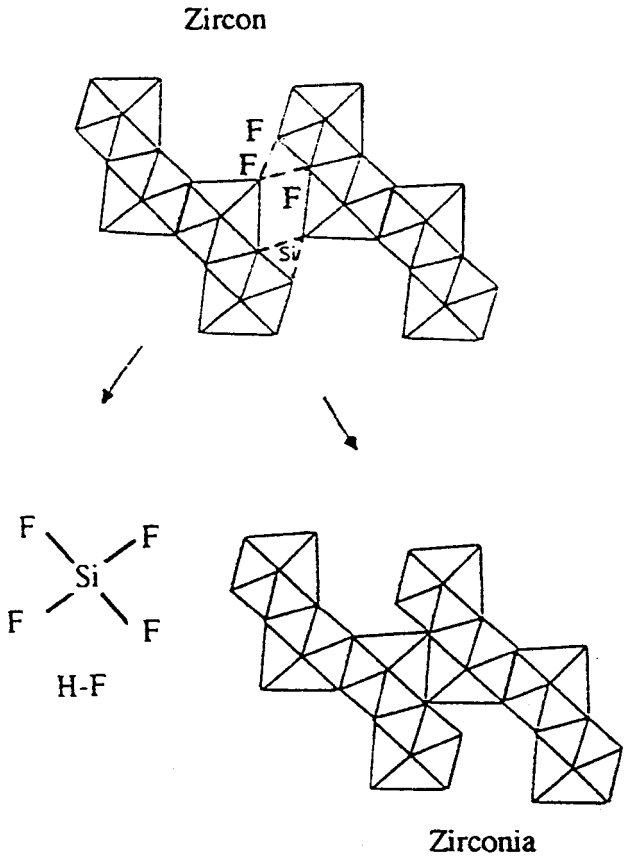

Fig. 15 Molar scale transformation of zircon A into zirconia in the lattice plane (200).

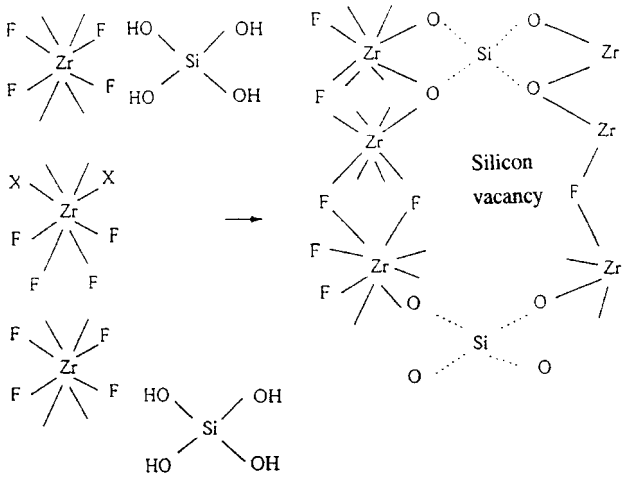

Fig. 16 Heterocondensation reaction leading to the formation of A type zircon.

cant fluoride concentrations, led to a new type of fluorinated zircon denoted 'zircon A' and characterised by the presence of silicon vacancies; the corresponding silica tetrahedra are replaced by tetrahedral nests $[F_n(OH)_{4-n}]$. The fluorine atoms are eliminated when samples are annealed at 750 °C, by evolution of hydrofluoric acid and silicon tetrachloride, and zircons A are irreversibly transformed into monoclinic zirconia exhibiting a plate-shaped morphology with an acicular network texture.

At the molecular level, transformation of zircon A into monoclinic zirconia could be considered as the narrowing of chains of zirconic dodecahedra in the (200) crystallographic planes with the destruction of silicic tetrahedra and hydroxy-fluoro nests involing the release of SiF_4 and HF (Fig. 15). Thus the relation between the orientation of zirconia stacks and the crystallographical directions of zircon platelets should be justified.

In the formation conditions of zircons A, the reactive dissolved species were identified as $Si(OH)_4$ and an octacoordinated zirconium monomeric entity including at least four fluorine atoms per zirconium atom. So, the heterocondensation reaction is likely to occur as shown in Fig. 16.

References

1 R. N. Singh, *J. Am. Ceram. Soc.*, 1990, **73**, 2399.
2 T. Mori, *J. Ceram. Soc. Jpn.*, 1990, **98**, 1017.
3 Y. Shi, X. X. Huang and D. S. Yan, *J. Eur. Ceram. Soc.*, 1994, **13**, 113.
4 M. H. Sainte Claire Deville and H. Caron, *Ann. Chim. Phys.*, 1865, **2**, 104.
5 Y. Kanno, *J. Mater. Sci.*, 1989, **24**, 2415.
6 T. Mori and Y. Yamamura, *J. Am. Ceram. Soc.*, 1992, **75**, 2420.
7 K. von Chrustchoff, *Sb. Mineral.*, 1892, **2**, 232.
8 C. Frondel and R. L. Colette, *Am. Mineral*, 1957, **42**, 759.
9 R. Caruba, A. Baumer and G. Turco, *Geochim. Cosmochim. Acta*, 1975, **39**, 11.
10 V. V. Sidorchuk and V. M. Certov, *Izv. Akad. Nauk SSSR, Georg. Mater.*, 1989, **25**, 622.
11 H. Kido and S. Kornarneni, *Trans. Mater. Res. Soc. Jpn.*, 1990, **1**, 358.
12 A. Mumptonf and R. Roy, *Geochim. Cosmochim. Acta*, 1961, **21**, 217.
13 A. Mosset, P. Baules, P. Lecante, J. C. Trombe, H. Ahamdane and F. Bensamka, *J. Mater. Chem.*, 1996, **6**, 1527.
14 R. Valéro, Ph.D. thesis, Université de Haute Alsace, France, 1997.
15 R. Valéro, B. Durand, J. L. Guth and T. Chopin, *Can. J. Chem.*, submitted.
16 R. Valéro, B. Durand, J. L. Guth and T. Chopin, *Can. J. Chem.*, submitted.
17 R. Valéro, B. Durand, J. L. Guth and T. Chopin, *Microporous Mesoporous Mater.*, submitted.
18 R. Caruba and G. Turco, *Bull. Soc. Fr. Min. Crist.*, 1971, **94**, 427.
19 I. A. Schneider and M. E. Roselli, *Am. Assoc. Quim. Argentina*, 1969, **57**, 59.
20 C. Alen, D. Larson and B. Robert, LANSKE, M5-HI 805, Los Alamos National Laboratory.
21 K. Robinson, C. V. Gibbs and P. H. Ribhe, *Am. Mineral.*, 1971, **56**, 782.
22 R. Valéro, J. L. Paillaud, B. Durand, J. L. Guth and T. Chopin, *J. Eur. Solid State Inorg. Chem.*, submitted.

Paper 8/05924A